DIFFUSE-INTERFACE METHODS IN FLUID MECHANICS

D. M. Anderson[1] *and G. B. McFadden*
Mathematical and Computational Sciences Division, National Institute of Standards and Technology, Gaithersburg, Maryland 20899; e-mail: mcfadden@nist.gov

A. A. Wheeler
Department of Mathematical Studies, University of Southampton, Highfield, Southampton, SO17 1BJ, United Kingdom; e-mail: aaw@maths.soton.ac.uk

ABSTRACT

We review the development of diffuse-interface models of hydrodynamics and their application to a wide variety of interfacial phenomena. These models have been applied successfully to situations in which the physical phenomena of interest have a length scale commensurate with the thickness of the interfacial region (e.g. near-critical interfacial phenomena or small-scale flows such as those occurring near contact lines) and fluid flows involving large interface deformations and/or topological changes (e.g. breakup and coalescence events associated with fluid jets, droplets, and large-deformation waves). We discuss the issues involved in formulating diffuse-interface models for single-component and binary fluids. Recent applications and computations using these models are discussed in each case. Further, we address issues including sharp-interface analyses that relate these models to the classical free-boundary problem, computational approaches to describe interfacial phenomena, and models of fully miscible fluids.

INTRODUCTION

The nature of the interface between two fluids has been the subject of extensive investigation for over two centuries. Young, Laplace, and Gauss, in the early part of the 1800s, considered the interface between two fluids to be represented

---

[1]Current address: Department of Mathematics, University of North Carolina, Chapel Hill, North Carolina 27599-3250; e-mail: dmanders@math.unc.edu

as a surface of zero thickness endowed with physical properties such as surface tension. In these investigations, which were based on static or mechanical equilibrium arguments, it was assumed that physical quantities such as density were, in general, discontinuous across the interface. Physical processes such as capillarity occurring at the interface were represented by boundary conditions imposed there (e.g. Young's equation for the equilibrium contact angle or the Young-Laplace equation relating the jump in pressure across an interface to the product of surface tension and curvature). Poisson (1831), Maxwell (1876), and Gibbs (1876) recognized that the interface actually represented a rapid but smooth transition of physical quantities between the bulk fluid values. Gibbs introduced the notion of a dividing surface (a *surface of discontinuity*) and surface excess quantities in order to develop the equilibrium thermodynamics of interfaces. The idea that the interface has a non-zero thickness (i.e. it is diffuse) was developed in detail by Lord Rayleigh (1892) and by van der Waals (1893), who proposed gradient theories for the interface based on thermodynamic principles. In particular, van der Waals gave a theory of the interface based on his equation of state and used it to predict the thickness of the interface, which he showed became infinite as the critical temperature is approached. Korteweg (1901) built on these ideas and proposed a constitutive law for the capillary stress tensor in terms of the density and its spatial gradients. These original ideas have been developed further and refined over the past century. For additional information, Rowlinson & Widom (1989) provide thorough discussions of the historical perspectives and complete references to the early work on interfacial and capillary phenomena.

The notion of a diffuse interface and the use of a capillary stress tensor to model the interface between two fluids and the forces associated with it are of central importance to the topics under consideration in this review. Our focus here is on the use of diffuse-interface models that fully couple these notions into a hydrodynamic description. Such models have been used to understand physical and hydrodynamic phenomena that occur near a fluid's critical point. Additionally, developments in modern computing technology have stimulated a recent resurgence in the use of the diffuse-interface models for the computation of flows associated with complex interface morphologies and topological changes, such as droplet breakup and coalescence, and the nonlinear development of classical hydrodynamic instabilities.

In the classical fluid mechanical approach, the interface between two immiscible fluids is modeled as a free boundary that evolves in time. The equations of motion that hold in each fluid are supplemented by boundary conditions at the free surface that involve the physical properties of the interface. This formulation results in a free-boundary problem (Lamb 1932, Batchelor 1967, Lighthill 1978, Drazin & Reid 1981, Davis 1983).

Specifically, in the free-boundary formulation it is assumed that the interface has a surface tension, which on applying a stress balance at the interface gives rise to the interfacial boundary condition

$$\boldsymbol{\sigma} \cdot \hat{n}|_{-}^{+} = \gamma \mathcal{K} \hat{n}, \tag{1}$$

which relates the jump in the stress across the interface to the interfacial curvature. Here $\boldsymbol{\sigma}$ is the stress tensor, $\hat{n}$ is the unit vector normal to the interface, γ is the surface tension (here assumed to be constant), and $\mathcal{K}$ is the appropriately signed mean curvature. In addition, an interface between two immiscible fluids is impermeable, in which case conservation of mass across the interface leads to

$$\vec{v} \cdot \hat{n}|_{-} = \vec{v} \cdot \hat{n}|_{+} = V_n, \tag{2}$$

where $\vec{v}$ represents the velocity of the fluid and V_n is the normal velocity of the interface. Finally, for viscous fluids, there is continuity of tangential velocity across the interface

$$[\vec{v} - (\vec{v} \cdot \hat{n})\hat{n}]|_{-}^{+} = 0. \tag{3}$$

The free-boundary description has been a successful model in a wide range of situations. However, there are also important instances where it breaks down. In short, as a physical model it breaks down when the interfacial thickness is comparable to the length scale of the phenomena being examined. For example, (*a*) in a near-critical fluid the thickness of the interface diverges at the critical point (Stanley 1971) and consequently the representation of the interface as a boundary of zero thickness may no longer be appropriate; (*b*) the motion of a contact line along a solid surface involves a detailed consideration of the fluid motion in the vicinity of the contact line and may require the treatment of length scales comparable to that of the interface thickness; and (*c*) the free-boundary description may not be adequate for situations involving changes in the topology of the interface (e.g. the breakup of a liquid droplet), since these processes fundamentally involve physical mechanisms acting on length scales comparable to the interface thickness. In addition to the above situations, another difficulty associated with the free-boundary formulation arises in its use in computational settings when the free boundary shape becomes complicated or self-intersecting.

Diffuse-interface models provide an alternative description in the face of these difficulties. Quantities that in the free-boundary formulation are localized to the interfacial surface are distributed throughout the interfacial region. For example, surface tension in the classical model is a representation of a distributed stress within the interfacial region. In this spirit a continuum theory of the interface may be developed where the reversible part of the stress tensor,

C, that is associated with surface tension is expressed in its simplest form as

$$C \propto \left(\rho \nabla^2 \rho + \frac{1}{2} |\nabla \rho|^2 \right) I - \nabla \rho \otimes \nabla \rho, \tag{4}$$

where ρ is the fluid density, I is the identity tensor, and the components of the outer product $\nabla \rho \otimes \nabla \rho$ are given by $(\partial \rho / \partial x_i)(\partial \rho / \partial x_j)$. Such a stress tensor, often called the capillary tensor, was described by Korteweg (1901). The derivatives of the density that appear in the stress tensor arise from the nonlocal interaction of the molecules within the interface. In this situation, the density ρ is the variable that distinguishes the bulk fluids and the intervening interface. In this role, it is known as the order parameter. In contrast, for a binary fluid undergoing spinodal decomposition, the composition c naturally plays the role of an order parameter (Cahn & Hilliard 1958). Alternatively it is possible that neither the density nor the composition may be an appropriate or convenient order parameter; such is the case in solidification models of single-component materials (e.g. Caginalp 1985, 1986, Langer 1986). Here it is possible to introduce an alternative order parameter, the so-called phase field ϕ, to characterize the phases. The phase-field assumes distinct constant values in each bulk phase and undergoes rapid but smooth variation in the interfacial region. The phase field can be regarded as a mathematical device that allows a reformulation of the free-boundary problem and has been used successfully in many instances. In particular, phase-field models of solidification have been used to compute complicated realistic interfacial structures such as those present during dendritic growth (Kobayashi 1993, Wheeler et al 1993, Warren & Boettinger 1995, Karma & Rappel 1997) and Ostwald ripening (Warren & Murray 1996).

Inherent in diffuse-interface models is an interfacial width that is characterized by the length scale over which the order parameter changes. By considering the asymptotic limit in which the interfacial width is small compared with the macroscopic length scale associated with the motion of the two bulk fluids (i.e. the sharp-interface limit), the diffuse-interface model can be related to the free-boundary problem.

In Section 2 we formulate the diffuse-interface theory of a single-component fluid near its critical point. Here we discuss developments for equilibrium and nonequilibrium situations and also review the applications addressed with this model. In Section 3 we review the developments of these ideas for a binary fluid. In Section 4 we discuss related topics, including the sharp-interface limit analyses, computational methods for fluid interfaces, and models of miscible fluids.

A SINGLE-COMPONENT FLUID

Diffuse-interface models of a single-component fluid have been developed largely from the perspective of critical phenomena. While they have been

used to study phenomena associated with the critical point, they have also been applied to situations away from the critical point. With this in mind, we review in this section the ideas and applications of diffuse-interface models of a single-component fluid.

Equilibrium

We begin by first considering the equilibrium state of a nonuniform single-component fluid. We assume that an isothermal fluid near its critical point has a Helmholtz free energy functional given by

$$\mathcal{F} = \int_V \left[\rho f(\rho, T) + \frac{1}{2} K |\nabla \rho|^2 \right] dV, \tag{5}$$

where V is a control volume, $f(\rho, T)$ is the bulk free energy density (per unit mass), K is a gradient energy coefficient (assumed for simplicity to be constant), and T is the temperature. In a simple model the term $\rho f(\rho, T)$ is assumed to take the form of a double well with respect to the density below the critical temperature and a single well above the critical temperature. The square-gradient term is associated with variations of the density and contributes to the free energy excess of the interfacial region, which defines the surface energy (Cahn & Hilliard 1958). The form of the energy density can be interpreted in the context of statistical mechanics in which the square gradient term arises from attractive long-ranged interactions between the molecules of the fluid and in which the gradient energy coefficient, K, can be related to the pair correlation function (for further details see Irving & Kirkwood 1950, Bearman & Kirkwood 1958, Yang et al 1976, Bongiorno et al 1976, Abraham 1979, de Sobrino & Peternelj 1982, and Davis & Scriven 1982).

The equilibrium conditions are obtained by minimizing $\mathcal{F}$ subject to a constraint of constant mass, $\mathcal{M}$, where

$$\mathcal{M} = \int_V \rho \, dV. \tag{6}$$

This leads to the Euler-Lagrange equation

$$K \nabla^2 \rho - (\rho f)_\rho + \lambda = 0, \tag{7}$$

where λ is the Lagrange multiplier associated with conservation of mass. The integrand of $\mathcal{F}$ as well as that of the mass constraint are independent of the spatial coordinates. Consequently, it follows from Noether's theorem (Goldstein 1980) that there is a corresponding conservation law given by

$$\nabla \cdot \boldsymbol{T} = 0, \tag{8}$$

where $\boldsymbol{T}$ is a second-rank tensor given by

$$\boldsymbol{T} = \mathcal{L}\,\boldsymbol{I} - \nabla\rho \otimes \frac{\partial\mathcal{L}}{\partial(\nabla\rho)}, \tag{9}$$

and $\mathcal{L} = \rho f(\rho, T) + \frac{1}{2}K|\nabla\rho|^2 - \lambda\rho$. Using the Euler-Lagrange equation (7) to eliminate the Lagrange multiplier we find that

$$\boldsymbol{T} = \left[-p + K\rho\nabla^2\rho + \frac{1}{2}K|\nabla\rho|^2\right]\boldsymbol{I} - K\nabla\rho \otimes \nabla\rho, \tag{10}$$

where $p = \rho^2 f_\rho$ has been identified as the thermodynamic pressure (e.g. see Callen 1985). Using the divergence theorem, Equation 8 may be expressed as

$$\int_S \boldsymbol{T} \cdot \hat{n}\,dA = 0, \tag{11}$$

where S is the boundary of a control volume with unit normal vector $\hat{n}$. This is the generalization to three dimensions of the first integral of the Euler-Lagrange Equation 7 in one dimension. Equations 8 and 11 suggest that $\boldsymbol{T}$ represents a stress tensor (up to an additive divergence-free contribution). We show in the next section that $\boldsymbol{T}$ represents the reversible part of the stress tensor. Similar equilibrium conditions have been obtained by Blinowski (1973a,b) from the point of view of elastic fluids. A review article covering a variety of aspects of this and related theories can be found in Davis & Scriven (1982). It was noted by Dunn & Serrin (1985) that consistency with nonequilibrium thermodynamics requires a more specific form for the capillary tensor than that used originally by Korteweg (1901), and later in the mechanical equilibrium theories of Aifantis & Serrin (1983a,b).

The equilibrium density profile $\rho(z)$ obtained using a van der Waals equation of state (Callen 1985, Rowlinson & Widom 1989) represents a smooth transition from one bulk density to the other (in the two-phase region) over a length scale associated with the gradient energy coefficient. Such an interface has a surface energy given by

$$\gamma = K \int_{-\infty}^{\infty} \left(\frac{d\rho}{dz}\right)^2 dz. \tag{12}$$

Nonequilibrium

We now pursue the nonequilibrium situation by outlining a thermodynamic procedure involving local balances of mass, linear momentum, energy, and entropy consistent with the inclusion of a square-gradient energy term in the internal energy functional. The total mass, $\mathcal{M}$, total momentum, $\vec{\mathcal{P}}$, total

internal energy, $\mathcal{E}$, and total entropy, $\mathcal{S}$, associated with a material volume $\Omega(t)$ are

$$\mathcal{M} = \int_{\Omega(t)} \rho \, dV, \tag{13a}$$

$$\vec{\mathcal{P}} = \int_{\Omega(t)} \rho \vec{v} \, dV, \tag{13b}$$

$$\mathcal{E} = \int_{\Omega(t)} \left(\frac{1}{2} \rho |\vec{v}|^2 + \rho e(s, \rho) + \frac{1}{2} K_E |\nabla \rho|^2 \right) dV, \tag{13c}$$

$$\mathcal{S} = \int_{\Omega(t)} \rho s \, dV, \tag{13d}$$

where $\vec{v}$ is the fluid velocity, e and s are the internal energy and entropy per unit of mass, respectively, and K_E is the gradient (internal) energy coefficient, which we assume to be constant. For simplicity, we have neglected body forces such as gravity. The associated physical balance laws can be expressed as

$$\frac{d\mathcal{M}}{dt} = 0, \tag{14a}$$

$$\frac{d\vec{\mathcal{P}}}{dt} = \int_{\delta\Omega(t)} \boldsymbol{m} \cdot \hat{n} \, dA, \tag{14b}$$

$$\frac{d\mathcal{E}}{dt} = \int_{\delta\Omega(t)} [\vec{v} \cdot \boldsymbol{m} \cdot \hat{n} - \vec{q}_E \cdot \hat{n}] \, dA, \tag{14c}$$

$$\frac{d\mathcal{S}}{dt} + \int_{\delta\Omega(t)} \vec{q}_S \cdot \hat{n} \, dA = \int_{\Omega(t)} \dot{s}^{prod} \, dV \geq 0, \tag{14d}$$

where $\delta\Omega(t)$ is boundary of $\Omega(t)$, $\boldsymbol{m}$ is the stress tensor, $\vec{q}_E$ and $\vec{q}_S$ are the internal energy and entropy fluxes, respectively, and $\dot{s}^{prod}$ is the volumetric entropy production. The quantities $\boldsymbol{m}$, $\vec{q}_E$, and $\vec{q}_S$, which in general include both classical and nonclassical contributions, are specified below such that their forms guarantee that $\dot{s}^{prod}$ is non-negative, as required by the Second Law of Thermodynamics. Equation 14a simply represents conservation of mass. Equation 14b states that the change in total momentum is related to the forces on the boundary (again note that we have neglected body forces). Equation 14c states that the change in total energy is related to the rate of working done by the forces on the boundary and also the energy flux through the boundary. Equation 14d states that the change in total entropy plus the entropy flux through the boundary must be equal to the entropy production. The definitions in Equation 13a–d and the balance laws in Equation 14a–d may

be manipulated to show that

$$\dot{s}^{prod} = \frac{(\boldsymbol{m} - \boldsymbol{T}) : \nabla \vec{v}}{T} + \left(\vec{q}_E + K_E \frac{D\rho}{Dt} \nabla \rho \right) \cdot \nabla \left(\frac{1}{T} \right)$$

$$+ \nabla \cdot \left(\vec{q}_S - \frac{\vec{q}_E}{T} - \frac{K_E}{T} \frac{D\rho}{Dt} \nabla \rho \right), \tag{15}$$

where $\boldsymbol{T}$ is the reversible part of the stress tensor given by Equation 10 with K replaced by K_E, and we have used the thermodynamic relationship $de = T ds + (p/\rho^2) d\rho$. The following specifications ensure that the entropy production is positive:

$$\boldsymbol{m} = \boldsymbol{T} + \boldsymbol{\tau}, \tag{16a}$$

$$\vec{q}_E = -k\nabla T - K_E \frac{D\rho}{Dt} \nabla \rho, \tag{16b}$$

$$\vec{q}_S = -\frac{k\nabla T}{T}, \tag{16c}$$

where k is the thermal conductivity and $\boldsymbol{\tau}$ is the viscous stress tensor given in the standard manner as $\boldsymbol{\tau} = \eta(\nabla \cdot \vec{v}) + \mu(\nabla \vec{v} + \nabla \vec{v}^T)$, where η and μ are coefficients of viscosity (e.g. Batchelor 1967). This prescription for $\boldsymbol{m}$ is similar to that postulated by Korteweg (1901). In this formulation it is assumed that the viscosity and thermal conductivity are, in general, functions of the density. We observe that the energy flux $\vec{q}_E$ involves both the classical contribution corresponding to the Fourier Law for heat conduction (Carslaw & Jaeger 1959, Kittel & Kroemer 1980) and a nonclassical contribution. This nonclassical contribution was referred to as interstitial working by Dunn & Serrin (1985), who also noted that there is no corresponding nonclassical term in the entropy flux. When a square-gradient term is included in the definition for total entropy (Equation 13d), a nonclassical entropy flux arises (e.g. Wang et al 1993, Wheeler et al 1996, Anderson & McFadden 1996). Using the above forms (Equation 16a–c) for the stress tensor and fluxes, the local balance laws may then be written as

$$\frac{D\rho}{Dt} = -\rho \nabla \cdot \vec{v}, \tag{17a}$$

$$\rho \frac{D\vec{v}}{Dt} = \nabla \cdot \boldsymbol{m}, \tag{17b}$$

$$\rho \frac{De}{Dt} = \nabla \cdot (k\nabla T) + (-p\boldsymbol{I} + \boldsymbol{\tau}) : \nabla \vec{v}, \tag{17c}$$

$$\rho T \frac{Ds}{Dt} = \nabla \cdot (k\nabla T) + \boldsymbol{\tau} : \nabla \vec{v}. \tag{17d}$$

These equations describe viscous, compressible, nonisothermal flow. To solve these it is necessary to supply an equation of state. In the isothermal situation, for example, one might specify the pressure p through a van der Waals equation of state.

This and similar models have been developed and studied by a number of authors from a variety of perspectives. Fixman (1967) developed a diffuse-interface hydrodynamic model in which the reversible part of the stress tensor was identified using a mechanical principle. In the model of Felderhof (1970), a more general form of the stress tensor was obtained that was compatible with the underlying Lagrangian. Langer & Turski (1973) derived a diffuse-interface model that they showed, through a coarse-graining argument, could be related to a molecular model. The model employed by Jasnow & Viñals (1996) was derived using a Hamiltonian description. Jacqmin (1996) described a model that also included a wall potential to model the interaction between the fluid and a solid boundary. Truskinovsky (1993) derived a similar model that also included an additional nonconserved order parameter and its gradients. Antanovskii (1996) presented a derivation of the model based on a maximum entropy principle. The derivation outlined above is most similar to that described by de Sobrino (1976), Dunn & Serrin (1985), Dunn (1986), and Anderson & McFadden (1996, 1997). The work of de Sobrino begins in a more general framework and invokes symmetry and invariance principles to simplify the gradient dependence of the stress tensor to that described above. Dunn & Serrin's approach is similar but mathematically more rigorous and is given from the viewpoint of rational mechanics.

A detailed numerical analysis of a simplified version of the diffuse-interface model has been performed by Affouf and Caflisch (1991), who present numerical solutions representing phase transitions, shocks, and rarefaction waves connecting far-field states, and analyze their stability.

Applications

CRITICAL POINT SCALING LAWS   Extensive analyses using renormalization-group techniques have been performed on a diffuse-interface model, commonly known in the literature as Model H (Hohenberg & Halperin 1977), which describes the dynamics of a binary fluid phase transition as well as a single-component fluid near its critical point (e.g. Halperin et al 1974, Siggia et al 1976, Hohenberg & Halperin 1977). Such analyses have identified divergent transport coefficients and scaling relations associated with near-critical fluids.

SHEAR FLOWS IN NEAR-CRITICAL FLUIDS   Onuki & Kawasaki (1979) and Onuki et al (1981) studied the dynamics of a near-critical fluid in a shear flow using a model developed by Kawasaki (1970). They investigated the regime

in which the equilibrium correlation length (i.e. the interfacial thickness) exceeds the length scale associated with the shear flow. They found that the critical fluctuations of classical fluids can be drastically altered (e.g. they can become highly anisotropic) by shear flows. These ideas have also been applied to polymers under shear flows (Helfand & Fredrickson 1989, Onuki 1989).

CAPILLARY WAVES   The diffuse-interface model has been used to study capillary waves (Felderhof 1970, Turski & Langer 1980, de Sobrino & Peternelj 1985, de Sobrino 1985). These authors began with a diffuse planar interface in equilibrium. They discussed capillary waves by means of a linearized theory about the equilibrium state. The linearized governing equations were examined in the long wavelength limit and the dispersion relation for capillary waves obtained from the classical free-boundary problem (e.g. Landau & Lifshitz 1959) is recovered. These authors recognized the importance of an isentropic treatment to the existence of capillary waves (in the context of a diffuse-interface model), although Felderhof derived the result in the isothermal case as well as under somewhat more restrictive conditions.

MOVING CONTACT LINES   Seppecher (1996) established the governing equations for an isothermal viscous flow near a moving contact line on a planar solid wall using a diffuse-interface model. In particular, a uniform distribution of double forces was used to describe the interaction between the fluid and the wall. In this analysis, the contact-line problem was separated into three regions: an external (outer) region far from the contact line where the classical theory of capillarity applies; an inner region very near the contact line whose dimensions are so small that the thickness of the interface cannot be neglected; and an intermediate region that matches the inner and outer regions. The flow in the inner region is compressible, while the flows in the intermediate and outer regions are incompressible. Examples of the density field and flow field in the inner region are shown in Figures 1 and 2. A key result of this paper was that the force singularity present in classical continuum models of moving contact lines (e.g. Huh & Scriven 1971, Dussan V & Davis 1974, Dussan V 1979) is not present when the interface is modeled as diffuse. This is attributed to mass transfer across the interfacial region. Additionally, numerical computations reveal a roughly linear increase in the apparent contact angle with the contact-line velocity (no contact-line hysteresis was considered), which agrees with the general trends observed experimentally (see Dussan V 1979). The moving contact-line problem has also recently been treated computationally by Jacqmin (1996) and is described in the next section.

INTERNAL WAVES IN A NEAR CRITICAL FLUID   Anderson & McFadden (1997) recently employed the diffuse-interface model to describe internal waves in
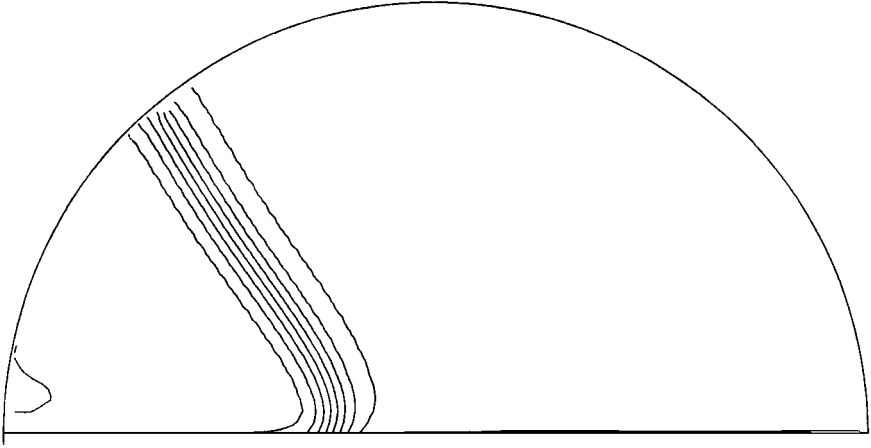
Figure 1   Moving contact line. This figure shows the constant density contours in the inner region. The frame of reference is fixed on the contact line region so that the bottom plate moves from left to right at an imposed velocity. In this case the imposed static contact angle at the wall is approximately 54°, while the dynamic contact angle (away from the immediate vicinity of the contact line) is approximately 125°. The parameter values consistent with the notation given in Seppecher (1996) are $R = 20$, $u_m = 2$, $K = 10$, $g = -0.3$, and $Ca = 40 \times 10^{-3}$. (Figure courtesy P Seppecher.)
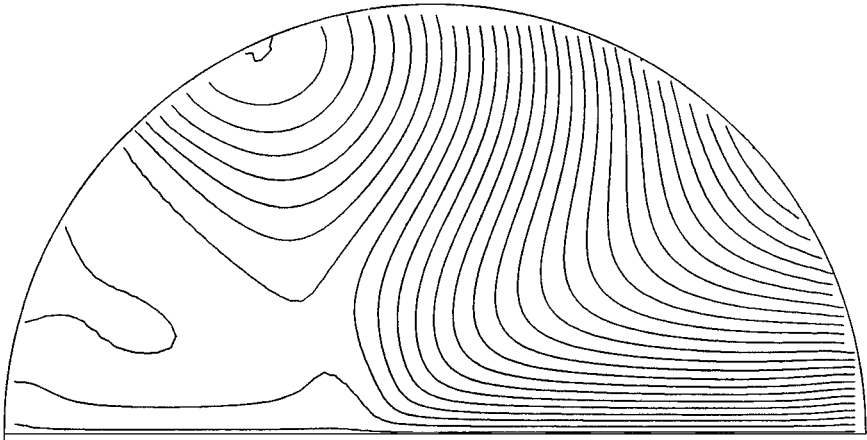

Figure 2   Moving contact line. This figure shows the streamlines in the inner region associated with the density contours shown in Figure 1. The frame of reference is fixed on the contact line region so that the bottom plate moves from left to right at an imposed velocity. (Figure courtesy P Seppecher.)

a near-critical fluid. These internal waves are present in small (centimeter-scale) containers owing to the large compressibility of the fluid near the critical point and have been observed experimentally in near-critical Xenon by Berg et al (1996). In the experimental work of Berg et al, internal gravity wave frequencies were measured both above the critical temperature where a single phase exists, and below the critical temperature where two phases, separated by an interface, exist. The theoretical development of Berg et al consisted of two separate models, one above the critical temperature and another below the critical temperature. In contrast to these classical hydrodynamic models, the diffuse-interface approach employed by Anderson & McFadden allows for a single model to be applied both above and below the critical temperature. In their diffuse-interface model, they use a van der Waals equation of state to obtain a base-state density profile. Upon this base-state, they introduce linear perturbations to calculate internal wave frequencies for temperatures both above and below the critical temperature. Predictions of the internal wave frequency from the diffuse-interface model are compared favorably with experimental data and theoretical results of Berg et al.

DROPLETS AND NUCLEATION   Several authors have investigated the nucleation of droplets (Blinowski 1974, Dell'Isola et al 1995, 1996). The focus of this work was to ascertain the effects of interfacial thickness on the nucleation conditions of a droplet, since at nucleation the droplet radius may be comparable to the interfacial thickness. Under these circumstances, the classical Laplace-Gibbs theory for the equilibrium radius of a droplet is called into question. Dell'Isola et al used an equilibrium formulation of a diffuse-interface model developed in earlier work (Dell'Isola & Kosiński 1993) to study nucleation of spherical droplets. In particular, they noted that for microscopic droplets the difference in mechanical pressures inside and outside the droplet (which is the quantity that is measured experimentally) is not the same as the difference between the thermodynamic pressures inside and outside the droplet. The mechanical pressure involves a (stress) contribution from the spatial density variation (e.g. the term in Equation 10 involving $\rho \nabla^2 \rho$), which at the center of the microscopic bubble is important. Based on these ideas, they carefully define quantities such as surface tension and droplet radius in a way that generalizes the classical notions. Relationships between surface tension, droplet radius, and the critical nucleation radius are obtained by using a number of different equations of state. Results for the minimal nucleation radius are compared with experimental measurements.

INSTABILITIES OF PLANAR JETS   Nadiga & Zaleski (1996) studied the inst-ability of a planar jet of viscous, compressible, isothermal liquid issuing into

its surrounding gas phase. They used a van der Waals equation of state to characterize the system. Their calculations focused on the high Reynolds number regime ($Re = 800$), and they investigated the effect of surface tension on the stabilization of the jet.

SPINODAL DECOMPOSITION IN A PURE FLUID   Nadiga & Zaleski (1996) also considered the spinodal decomposition of a single-component fluid rapidly quenched from a temperature above its critical point to a temperature below the critical point. These computations are isothermal and two-dimensional. They found that the inclusion of hydrodynamic effects in the model leads to a predicted growth rate that is slightly enhanced from the case of diffusion-limited growth. Numerical computations show the domain growth, and plots of domain size versus time are presented.

A BINARY FLUID

Nonequilibrium

We now consider the situation of a binary fluid consisting of two components, A and B. We denote the composition of component A, expressed as a mass fraction, by c. In this setting the composition plays the role of an order parameter that distinguishes the different phases of the fluid and in this way is analogous to the density in the single-component fluid models. However, a number of subtle differences exist between the single-component and binary fluid models.

The governing equations for the flow of a nonisothermal, compressible binary fluid may be developed in a manner similar to those for the single-component case discussed above, but involve square-gradient contributions in the internal energy functional from the composition rather than from the density. This procedure leads to an expression for entropy production of the form

$$\dot{s}^{prod} = \frac{(\boldsymbol{m} - \boldsymbol{T}_C) : \nabla \vec{v}}{T} + \left(\vec{q}_E + K_E \frac{Dc}{Dt} \nabla c \right) \cdot \nabla \left(\frac{1}{T} \right)$$

$$- \vec{q}_C \cdot \nabla \left(\frac{\mu_c}{T} \right) + \nabla \cdot \left(\vec{q}_S - \frac{\vec{q}_E}{T} - \frac{K_E}{T} \frac{Dc}{Dt} \nabla c + \mu_c \vec{q}_C \right), \qquad (18)$$

where $\boldsymbol{T}_C$ is the reversible part of the stress tensor given by

$$\boldsymbol{T}_C = \left(-p + \frac{1}{2} K_E |\nabla c|^2 \right) \boldsymbol{I} - K_E \nabla c \otimes \nabla c, \qquad (19)$$

$\vec{q}_C$ is the mass flux of component A, and μ_c is the generalized chemical potential given by

$$\mu_c = \frac{\partial e}{\partial c} - \frac{K_E}{\rho} \nabla^2 c. \qquad (20)$$

The specification of $\boldsymbol{m}$, $\vec{q}_E$, $\vec{q}_S$, and $\vec{q}_C$ to ensure positive entropy production follows in an analogous way to the single-component case. In particular, $\vec{q}_C = -D\nabla(\mu_c/T)$, where D is positive and represents the diffusion coefficient. Consequently, the equation for the composition is given by

$$\rho\frac{Dc}{Dt} = \nabla \cdot \left\{ D\nabla \left[\frac{1}{T} \left(\frac{\partial e}{\partial c} - \frac{K_E}{\rho}\nabla^2 c \right) \right] \right\}. \tag{21}$$

This is the well-known Cahn-Hilliard equation, used to model spinodal decomposition by Cahn (1961) and Hilliard (1970), modified to account for fluid motion. The equations governing density, velocity, and temperature (energy) are similar to those for a single-component fluid given above by Equations 17a–d. Two subtle differences between the binary fluid equations and the single-component fluid equations are worth mentioning. First, the reversible part of the stress tensor $\boldsymbol{T}_C$ does not contain the counterpart of the Laplacian term appearing in $\boldsymbol{T}$ (see Equation 10). This is because the order parameter c is given per unit mass in contrast to the density ρ. Second, the order parameter c is governed by the modified Cahn-Hilliard equation (Equation 21), whereas the density ρ is governed by the continuity equation (Equation 17a).

Details of the derivation of the governing equations for a binary fluid have been discussed by a number of authors. Blinowski (1975) considered the binary fluid case, and also more general multi-component systems. Starovoitov (1994) derived a binary fluid diffuse-interface model using a virtual power method. Antanovskii (1995) derived the equations for nonisothermal, viscous, quasi-compressible flow. His derivation was based on a maximum entropy principle, similar to the approach described here, but used virtual work arguments to identify the forms of the stress tensor and fluxes. Gurtin et al (1996) derived a model for an isothermal, incompressible flow using microforce balance laws. Jasnow & Viñals (1996) illustrated the derivation of the equations for a binary fluid using a Hamiltonian formalism. Although their derivation was given for an isothermal, inviscid, incompressible fluid, the model was extended to the case where the fluid was viscous and the temperature field varied slowly in time. A similar account can be found in Jacqmin (1996), who discussed the model in a potential form as well as making note of its relation to the above stress form. The merits of these two equivalent formulations were discussed in terms of specific applications. Lowengrub & Truskinovsky (submitted for publication) presented a thorough derivation of the diffuse-interface model based on entropy production and paid particular attention to the difference between compressible and quasi-incompressible fluids. The quasi-incompressible situation describes the case where the fluid density is independent of the pressure. However, the bulk states may have different densities and the flow in the interfacial region is in general nonsolenoidal ($\nabla \cdot \vec{v} \neq 0$), resulting in an expansion or contraction flow upon

phase transformation. These authors argued that within the context of quasi-incompressibility, the appropriate thermodynamic description is in terms of a Gibbs free energy, in which the pressure is an independent variable determined by the transport equations rather than a quantity determined thermodynamically.

Applications

THERMOCAPILLARY FLOWS   Antanovskii (1995) used his nonisothermal binary fluid model to compute one-dimensional thermocapillary flow in a gap. In this situation, two fluid phases, characterized by their different compositions, were separated by a planar diffuse interface along which a temperature gradient was imposed. Calculations for different values of interfacial layer thickness and viscosity ratios were presented. Jasnow & Viñals (1996) investigated thermocapillary migration of droplets of one phase in the surrounding phase. They focused on drops with radii on the order of ten times the correlation length. Their calculations show the motion of the droplet through the temperature gradient as a function of time, and the dependence of its velocity on this temperature gradient. Also shown is a sequence in which two droplets coalesce.

SPINODAL DECOMPOSITION   Gurtin et al (1996) considered spinodal decomposition occurring in an isothermal binary fluid. Their computations, which began with an initial random distribution of the composition, showed the coarsening process explicitly. They noted that the main effect of the hydrodynamic interactions on this process is the flow-induced coalescence of droplets. Their calculations specifically show the flow associated with these coalescence phenomena. They computed the domain (structure) size, compared with classical predictions, and found that for long times the growth is faster than the classical scaling law for coarsening by purely diffusive mechanisms. Jasnow & Viñals (1996) considered a similar situation but included the effects of a nonuniform temperature field. Their results, displayed in the time-sequence in Figure 3, show the spinodal decomposition of a binary fluid in a rectangular cell across which a vertical temperature gradient is imposed (the cell is hottest at the bottom). Here, an initially random composition distribution (Figure 3, *top*) undergoes coarsening and domain growth. At an intermediate time (*middle*) and a later time (*bottom*), their calculations show nonuniform coarsening wherein the smaller (larger) scales occur in the warmer (cooler) regions.

MIXING AND INTERFACIAL STRETCHING   Chella & Viñals (1996) computed the mixing and interfacial stretching of an isothermal, incompressible binary fluid in a shear flow with equal densities and viscosities in the two phases. An initially planar interface distorted under an imposed shear flow. The wrapping up of the two phases is shown for different values of the capillary number (surface energy). The amount of interfacial stretching was computed and compared with
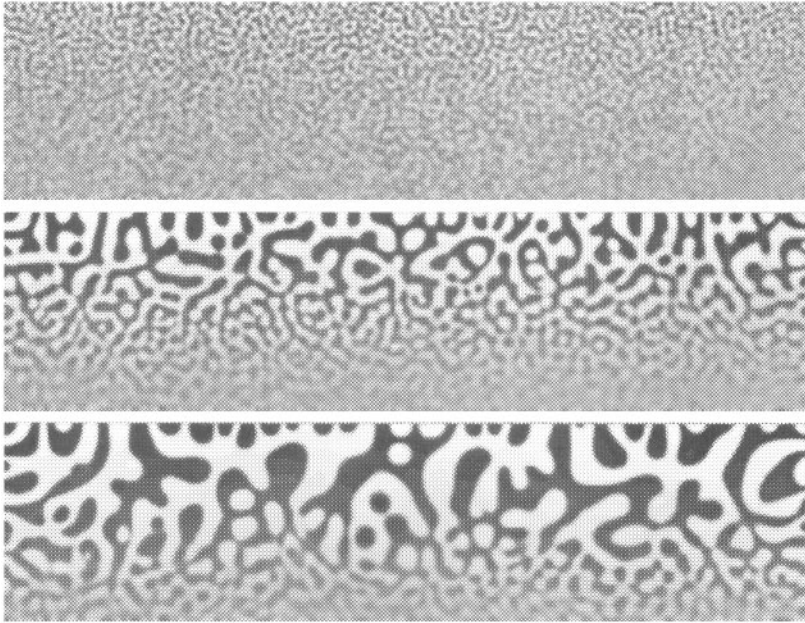
Figure 3   Spinodal decomposition. This time sequence (*top* to *bottom*) shows spinodal decomposition of a binary fluid in a rectangular cell across which is imposed a vertical temperature gradient (the cell is hottest at the *bottom*). The composition is indicated in *grayscale*. These computations show the system evolving from an initially random composition distribution (*top*), to one wherein the domain structure size varies with the temperature (*bottom*).   (Figure courtesy D Jasnow & J Viñals.)

an analytical solution for that associated with a passive scalar. An increase in the surface energy corresponded to a decrease in the amount of stretching and in this way opposed the effect of the shear flow. Further calculations by Chella and Viñals of flow in a driven cavity are shown in Figure 4. A number of breakup and coalescence events can be seen in this sequence.

DROPLET BREAKUP   Jacqmin (1996) calculated the breakup of an inviscid fluid in the context of a two-dimensional isothermal model. The initially elongated droplet relaxes, oscillates, and breaks apart into two separate droplets. In these calculations, the diffusion coefficient (D in our notation) was made velocity-dependent. In addition to plots showing the actual droplet breakup process, the kinetic and surface energy evolutions are also given. In the case where the flow is strongly damped by using a larger value of D, the energy of the droplet decreases rapidly and breakup does not occur.
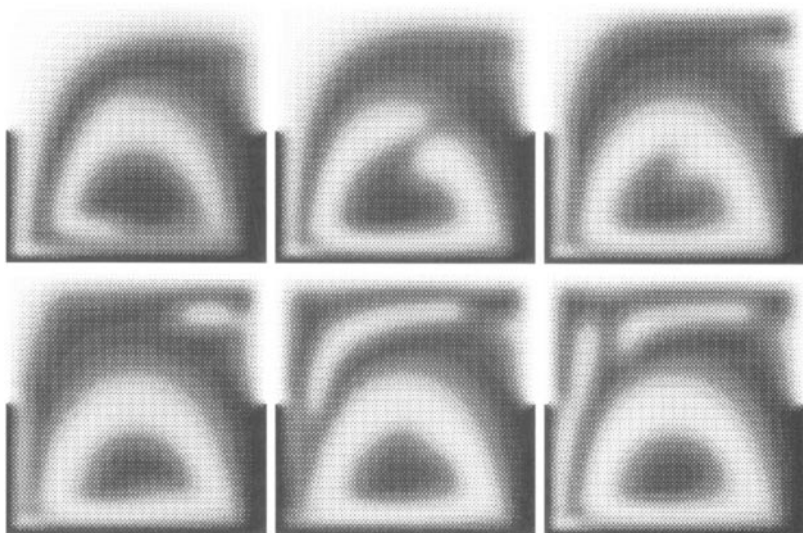
Figure 4   Flow in a driven cavity. This time sequence (*top* and *bottom*, *left* to *right*) shows the order parameter (*grayscale*) representing the binary fluid composition. The flow is set up by an imposed velocity (*left* to *right*) on the bottom surface of the cavity. The densities and viscosities of both phases are equal. (Figure courtesy R Chella & J Viñals.)

WAVE-BREAKING AND SLOSHING   Jacqmin (1996) also applied the diffuse-interface model to a large-deformation sloshing flow in a two-dimensional rect-angular domain. Interaction with the solid wall of the container was modeled by using a wall potential associated with a 90° contact angle between the wall and the interface. The two-phase fluid in a uniform (vertical) gravitational field was subjected to an oscillating horizontal acceleration whose amplitude increased linearly in time. The motion of the initially planar interface between the two stably stratified phases was computed once the horizontal accelerations began. The shape of the interface became highly nonlinear and several breakup and coa-lescence events occurred. It was noted that the prediction of coalescence events may occur more quickly than is physically realistic, because a high level of accu-racy is needed to resolve the draining layer between the two coalescing phases.

MOVING CONTACT LINES   Jacqmin (1996) investigated the fluid motion near a moving contact line. These steady calculations show the existence of a dynamic contact angle associated with the interface away from the immediate vicinity of the contact line. Also observed is a streamline—similar to that observed in the experiments by Dussan V & Davis (1974)—issuing from the contact line region into the displaced fluid.

NUCLEATION   Lowengrub & Truskinovsky (submitted for publication) considered nucleation (and annihilation) of an isothermal, spherically symmetric equilibrium droplet. In particular, they used the diffuse-interface model to describe the situation where the droplet size was comparable to the interface thickness. In the incompressible case, where the density was uniform everywhere, they performed an analysis of the spherically symmetric Cahn-Hilliard equation with a free-energy density composed of piecewise parabolas to find analytic solutions for the compositions. In the compressible case, they proceeded numerically and concluded from their results that compressibility has little effect on the interfacial structure of the droplet.

RELATED TOPICS

Sharp-Interface Limit

As noted in the section on a single-component fluid, the diffuse-interface models may be applied away from the critical point, where the interfacial thickness approaches that of a sharp boundary. The use of the diffuse-interface models in these regimes may be justified by demonstrating that they approach asymptotically the free-boundary formulation. This is achieved by adopting what is commonly known as the sharp-interface limit.

In the context of phase-field models of solidification, there has been significant effort to address the sharp-interface limit and to compare the model to well-known results of the free-boundary problem (e.g. Caginalp 1989, Braun et al 1994).

A key feature in the diffuse-interface models described here, which is not present in the phase-field solidification models studied to date, is the (vector) momentum equation that involves the distributed capillary stresses. Consequently, much of the emphasis in terms of the sharp-interface analyses of the diffuse-interface model has been to recover the classical interfacial boundary conditions associated with the stress balance at the interface. Here we describe the efforts in this area and outline a simple reduction of the momentum balance to the interfacial stress jump using a pillbox argument.

From his diffuse-interface model of a binary fluid, Antanovskii (1995) derived the special cases of the classical hydrostatic balance for a flat interface in equilibrium and the Young-Laplace equation for a spherical interface in equilibrium. The latter case has also been considered for a single-component model by Blinowski (1979). Nadiga & Zaleski (1996) also confirmed numerically that their diffuse-interface model accurately recovered the classical results for a flat interface and for a liquid droplet in equilibrium. Jasnow & Viñals (1996) derived from the capillary term in their momentum equation the appropriate sharp-interface tangential and normal forces when the surface

tension was a slowly varying function along the interface. More detailed analytical approaches have been addressed by Starovoitov (1994), Anderson & McFadden (1996), and Lowengrub & Truskinovsky (submitted for publication).

To illustrate these ideas, we apply a pillbox argument to the momentum balance (Equation 17b) to show how the classical stress balance at a fluid-fluid interface can be derived from the diffuse-interface model. We define a small parameter ϵ measuring the thickness of the interface by $K_E = \epsilon^2 \bar{K}$. We then consider the surface S_I defined by the contour of density upon which the interfacial region collapses in the limit $\epsilon \to 0$ and define a pillbox enclosing a portion of this surface at a fixed point in time in such a way that the top of the pillbox is above the surface at a height $r = \delta$ and the bottom of the pillbox is below the surface at a height $r = -\delta$. Here, r is a local coordinate normal to the interface. The key limit in the pillbox argument is that $\epsilon \ll \delta \ll L$, where L is a length scale associated with the outer flow. In this limit, the volume of the pillbox becomes negligible on the outer scales, but the variations in the density, which define the interfacial region, occur over a region fully contained within the pillbox. Also in this limit, the unit normal vectors on the top and bottom of the pillbox are $\hat{n}$ and $-\hat{n}$, respectively, while the unit normal on the side is given by $\hat{m}$ (note that $\hat{m} \cdot \hat{n} = 0$).

We integrate Equation 17b to obtain

$$0 = \int_{V_p} \left(\frac{\partial(\rho\vec{v})}{\partial t} + \nabla \cdot (\rho\vec{v} \otimes \vec{v}) - \nabla \cdot \boldsymbol{m} \right) dV, \tag{22}$$

where we have used Equation 17a, and the fact that

$$\rho \frac{D\vec{v}}{Dt} = \frac{\partial(\rho\vec{v})}{\partial t} + \nabla \cdot (\rho\vec{v} \otimes \vec{v}). \tag{23}$$

Next, we note that

$$\int_{V_p} \frac{\partial(\rho\vec{v})}{\partial t} dV \to - \int_{S_p} (\rho\vec{v})\vec{v}_I \cdot \hat{n}_S \, dS, \tag{24}$$

where $\vec{v}_I$ is the velocity of the surface S_I described above, and S_p denotes the surface of the pillbox. This result follows by translating to a frame moving with the interface so that $\partial(\rho\vec{v})/\partial t = \partial(\rho\vec{v})/\partial t' - \vec{v}_I \cdot \nabla(\rho\vec{v}) = \partial(\rho\vec{v})/\partial t' - \nabla \cdot (\rho\vec{v}_I \otimes \vec{v}) + \rho\vec{v}\nabla \cdot \vec{v}_I$. The terms $\partial(\rho\vec{v})/\partial t' + \rho\vec{v}\nabla \cdot \vec{v}_I$ are bounded and hence do not contribute as the pillbox volume goes to zero. We use this and the divergence theorem to obtain from Equation 22

$$0 = \int_{S_p} [\rho\vec{v}(\vec{v} - \vec{v}_I) \cdot \hat{n}_S - \hat{n}_S \cdot \boldsymbol{m}] \, dS. \tag{25}$$

We further argue that the fluid velocity terms are bounded (so that they do not contribute to the integral over the side surface of the pillbox), and that the

nonclassical terms do not contribute to the upper and lower surfaces of the pillbox (because $\epsilon \ll \delta$) so that

$$0 = \int_A [\rho \vec{v}(\vec{v} - \vec{v}_I) \cdot \hat{n} - \hat{n} \cdot (-p \, \boldsymbol{I} + \, \boldsymbol{\tau})]^+_- dA - \int_{side} \hat{m} \cdot \boldsymbol{T} dS, \qquad (26)$$

where A is the portion of S_I within the pillbox. Local to the interfacial region we have $\nabla \rho \sim \rho_r \hat{n}$ and $\nabla^2 \rho \sim \rho_{rr}$ to leading order. Then $\hat{m} \cdot \boldsymbol{T} \sim (\hat{m} \cdot \boldsymbol{T} \cdot \hat{m})\hat{m}$ so that

$$0 = \int_A [\rho \vec{v}(\vec{v} - \vec{v}_I) \cdot \hat{n} - \hat{n} \cdot (-p \, \boldsymbol{I} + \, \boldsymbol{\tau})]^+_- dA$$

$$- \oint_C \int_{-\infty}^{\infty} (\hat{m} \cdot \boldsymbol{T} \cdot \hat{m})\hat{m} \, dr \, dl, \qquad (27)$$

where C is the contour defined by the intersection of S_I, and the pillbox surface and dl is the increment of arclength along C. We next define the scalar

$$\gamma = \int_{-\infty}^{\infty} (\hat{m} \cdot \boldsymbol{T} \cdot \hat{m}) dr, \qquad (28)$$

which can be shown to be equal to the excess Kramer's potential, that is, the surface energy (Anderson & McFadden 1996). We then apply the surface divergence theorem (Weatherburn 1925), which allows us to write

$$\oint_C \gamma \hat{m} dl = \int_A [\nabla_S \gamma - \gamma \, (\nabla_S \cdot \hat{n}) \, \hat{n}] \, dA, \qquad (29)$$

where $\nabla_S \gamma$ is the surface gradient of γ, and $\nabla_S \cdot \hat{n}$, the surface divergence of $\hat{n}$, is the interfacial curvature, $\mathcal{K}$. This gives

$$0 = \int_A \left\{ [\rho \vec{v}(\vec{v} - \vec{v}_I) \cdot \hat{n} - \hat{n} \cdot (-p \, \boldsymbol{I} + \, \boldsymbol{\tau})]^+_- - [\nabla_S \gamma - \gamma \mathcal{K} \hat{n}] \right\} dA. \qquad (30)$$

Finally, noting that the area of integration is arbitrary yields

$$[\rho \vec{v}(\vec{v} - \vec{v}_I) \cdot \hat{n} - \hat{n} \cdot (-p \, \boldsymbol{I} + \, \boldsymbol{\tau})]^+_- = \nabla_S \gamma - \gamma \mathcal{K} \hat{n}, \qquad (31)$$

which is the classical stress balance at a fluid-fluid interface (Delhaye 1974). Note that the first term on the left-hand side represents a jump in the momentum across the interface and is zero when there is no mass flux across the interface.

Other Computational Methods

The diffuse-interface models share common features with a number of methods developed from a more computational point of view. We outline several of these methods below and highlight some of their applications.

The volume of fluid (VOF) method (Hirt & Nichols 1981, Hyman 1984, Tsai & Yue 1996) is a numerical approach to the free-boundary problem in which an auxiliary function F, which distinguishes one fluid from another, is introduced in order to identify the shape and evolution of the free boundary. This function satisfies $DF/Dt = 0$; that is, it is advected with the flow. Each computational cell has associated with it a value of F, and those cells that take on a value between two bulk values of F are assumed to contain part of the interface. The normal to the interface in the cell is determined by the direction of the largest local gradient, and the position of the interface in the cell is arranged so that F is the fractional volume of fluid in the cell. The VOF method, like the diffuse-interface approach, allows a straightforward description of flows involving complicated boundary shapes and topological changes. In contrast to the diffuse-interface approach, however, free surface boundary conditions in the VOF method must still be applied at the free boundary.

Brackbill et al (1992) developed a continuum surface force model wherein they identified a volume force that represents surface tension spread over a small but finite three-dimensional interfacial domain. This volume force was related to a *color* function that, for example, can represent density for incompressible flows. The defining characteristics of this volume force are that it gives the correct surface force in the limit of a sharp interface and is nonzero only in the interfacial region. This approach allows a single-domain description of the two-fluid system and does not require the direct application of boundary conditions, which are built into the governing equations.

A number of numerical results are presented for both static and dynamic situations: (*a*) a static drop (rod), (*b*) a nonequilibrium rod upon which capillary waves move along the surface, (*c*) the Rayleigh-Taylor instability and the associated interfacial deformation, (*d*) flow induced by wall-adhesion whereby the fluid conforms to an imposed equilibrium contact angle on the wall, and (*e*) jet-induced tank mixing and liquid reorientation in microgravity environments.

Another related approach was developed by Unverdi & Tryggvason (1992a,b), who used a front-tracking technique employing a numerically diffuse description of the interface. They constructed an indicator function, based on the known position of the (sharp) interface, that identified fluid properties such as density and viscosity. This function was then artificially spread out over a small region on the scale of the computational mesh size, allowing the fluid properties to vary smoothly through this interfacial region. The surface force (i.e. surface tension) was also distributed over this interfacial region so that a single-domain approach could be used to calculate the flow. This flow then determined how the interface was advected. In Unverdi & Tryggvason (1992a), both two- and three-dimensional multiple bubble motion and interaction were presented. In Unverdi & Tryggvason (1992b), the Rayleigh-Taylor instability in two and

three dimensions and also bubble-bubble interaction in three dimensions were computed.

Nobari et al (1996) recently used this approach to compute head-on collision of two viscous liquid droplets with surface tension. Here, rupture was modeled by artificially removing the thin film between the two drops at a prescribed time. They found that if no rupture takes place, the drops rebound, but that when rupture occurs the drops may later split. This method was extended by Juric & Tryggvason (1995, 1996, 1997) to describe flows in the presence of phase change. Here, they applied the model to vapor bubble dynamics and film boiling.

Another highly successful computational scheme applied to interfacial motion is the level-set method (Osher & Sethian 1988, Sethian 1996). With this method, the interface is represented as a level set of a smooth auxiliary function that is computationally analogous to the order parameter used in diffuse-interface descriptions. An advantage of the level-set method is that the interface remains sharp in this formulation, which eliminates the need for added numerical resolution in the direction normal to the interface. Within the context of fluid mechanics and two-fluid flows, surface tension, for example, is represented in the momentum equations as a distributed force through the use of a smoothed delta-function (Sussman et al 1994, Chang et al 1996). The momentum equations are then used to compute the flow over the whole domain and the level-set function is advected with the flow. After a normalization procedure, the level-set function determines the new position of the interface.

Mulder et al (1992) applied the level-set approach (without surface tension) to study the Rayleigh-Taylor and Kelvin-Helmholtz instabilities within the context of compressible gas dynamics. Sussman et al (1994) used this approach to model incompressible two-dimensional rising bubbles and falling drops, which show large distortions and topological changes. They also show two impacting droplets as well as a single droplet impacting a surface. Chang et al (1996) also applied a level-set approach for incompressible fluids to several topologically complex flows. They presented computations of two merging fluid bubbles of equal density and also two merging fluid bubbles of different density. Further, they investigated the Rayleigh-Taylor instability of an initially motionless, vertical column of fluid and showed calculations of the subsequent vortex sheet roll-up phenomena.

Miscible Fluids

The ideas that are involved in the diffuse-interface models described in the preceding sections are similar in many ways to those for miscible fluids. In particular, fluid stresses (i.e. Korteweg, or capillary, stresses) that arise as a result of concentration and density gradients at the interface between two miscible fluids lead to the notion of surface tension between miscible fluids. Joseph (1990) investigated these ideas both experimentally and theoretically.

He performed a number of experiments and highlighted other experimental work in which miscible liquid droplets rising or falling in another liquid exhibit capillary-type effects; that is, their shapes are consistent with the presence of surface tension on the interface. In the theoretical development, the equations governing the motion of the fluid are similar to those presented above on binary fluids. They are the continuity equation, the Navier-Stokes equations modified to account for the gradient stresses, the heat (energy) equation, and a standard diffusion equation, rather than the modified Cahn-Hilliard equation (Equation 21), which describes the evolution of the composition.

Besides the difference in the equations governing the composition, another key difference between the description given by Joseph (1990) and that for a binary fluid is that his model described a generalized (or quasi-) incompressible fluid. Here it is assumed that the density is a function of composition and temperature but is independent of the pressure. Although the density then is unchanged by pressure variations, the associated flow may still be nonsolenoidal ($\nabla \cdot \vec{v} \neq 0$) because of composition or temperature variations. This notion has been carefully adopted into the diffuse-interface model for a binary fluid by Lowengrub & Truskinovsky (submitted for publication).

The theoretical model described by Joseph (1990) was analyzed in more detail by Galdi et al (1991). These authors reworked the equations and identified a new solenoidal velocity, which is a linear combination of the original velocity field and the concentration gradient. Associated with this new velocity is a pressure field that is a linear combination of the original pressure and the divergence of the original velocity. They addressed the linear and energy stability of a quiescent, vertically (unstably) stratified incompressible fluid in which Korteweg stresses arise because of composition gradients. This is the analog of the classical Bénard problem, with the exception that the authors do not immediately invoke the Boussinesq approximation. They found that the stability results depended strongly on the value of the coefficient in the Korteweg stress (and in particular on its sign). When its sign is chosen consistent with that in the capillary stress term described in the section on a single-component fluid, and when its effect is strong enough, an unconditionally stable base state is predicted.

A notable idea described in the paper by Joseph (1990) is that of a dynamic (or nonequilibrium) surface tension between two miscible fluids. That is, although for two miscible fluids it is not clear that one can define an equilibrium surface tension, based on the idea of stresses associated with gradients in density or composition, transient or dynamic surface tension between two mixing phases can be studied. Joseph et al (1996) consider this situation in detail. In that paper, they carried out an analysis using the model of Joseph (1990) of transient or dynamic interfacial tension during the smoothing of an initial discontinuity of composition across plane and spherical surfaces separating two miscible liquids. They found that the dynamic interfacial tension decays in time like $t^{-1/2}$ and

had contributions from Korteweg stresses and from the expansion velocity (i.e. the nonsolenoidal part), which also involved the rate of change of viscosity with composition. For a plane mixing front, diffusion had a similarity solution, and they showed that there is no associated pressure jump resulting from the Korteweg terms (i.e. surface tension does not lead to a jump in pressure when the curvature of the interface is zero). The only pressure difference across the mixing front was due to the hydrostatic pressure difference (i.e. due to gravity) across the layer because its thickness grew with time. For an initially spherical droplet placed in another (miscible) fluid, they identified a pressure jump associated with two effects: The first is due to the Korteweg stress and the second is due to the expansion velocity and is proportional to the rate of change of viscosity with composition. The latter term can take on either sign, depending on the assumed composition-dependence of the viscosity.

SUMMARY

We reviewed the development and application of diffuse-interface models for both single-component and binary fluids. These models have foundations in statistical mechanics, kinetic theory, mechanical theories, and nonequilibrium thermodynamics. They provide an alternative approach to the classical hydrodynamic free-boundary problem and have been used successfully in many applications. They should continue to play an important role, in concert with other theoretical and experimental efforts, in the understanding of hydrodynamic phenomena associated with critical fluids and other flows involving complex interface morphologies and topological changes.

Literature Cited

Abraham FF. 1979. On the thermodynamics, structure and phase stability of the nonuniform fluid state. *Phys. Rep.* 53:93–156

Affouf M, Caflisch RE. 1991. A numerical study of Riemann problem solutions and stability for a system of viscous conservation laws of mixed type. *SIAM J. Appl. Math.* 51:605–34

Aifantis EC, Serrin JB. 1983a. Equilibrium solutions in the mechanical theory of fluid microstructures, *J. Colloid Int. Sci.* 96:530–47

Aifantis EC, Serrin JB. 1983b. The mechanical theory of fluid interfaces and Maxwell's rule. *J. Colloid Int. Sci.* 96:517–29

Anderson DM, McFadden GB. 1996. A diffuse-interface description of fluid systems. *NIST Int. Rep. 5887.* Gaithersburg, MD: NIST

Anderson DM, McFadden GB. 1997. A diffuse-interface description of internal waves in a near-critical fluid. *Phys. Fluids* 9:1870–79

Antanovskii LK. 1995. A phase-field model of capillarity. *Phys. Fluids* 7:747–53

Antanovskii LK. 1996. Microscale theory of surface tension. *Phys. Rev. E* 54:6285–90

Batchelor GK. 1967. *An Introduction to Fluid Dynamics.* Cambridge: Cambridge Univ. Press

Bearman RJ, Kirkwood JG. 1958. Statistical mechanics of transport processes. XI. Equations of transport in multicomponent systems. *J. Chem. Phys.* 28:136–45

Berg RF, Lyell MJ, McFadden GB, Rehm RG. 1996. Internal waves in xenon near the critical point. *Phys. Fluids* 8:1464–75

Blinowski A. 1973a. On the order of magnitude of the gradient-of-density dependent part of an elastic potential in liquids. *Arch. Mech.* 25:833–49

Blinowski A. 1973b. On the surface behavior of gradient-sensitive liquids. *Arch. Mech.* 25:259–68

Blinowski A. 1974. Droplets and layers in the gradient model of a capillary liquid. *Arch. Mech.* 26:953–63

Blinowski A. 1975. Gradient description of capillary phenomena in multicomponent fluids. *Arch. Mech.* 27:273–92

Blinowski A. 1979. On two phenomenological models of capillary phenomena. *Arch. Mech.* 31:423–30

Bongiorno V, Scriven LE, Davis HT. 1976. Molecular theory of fluid interfaces. *J. Coll. Int. Sci.* 57:462–75

Brackbill JU, Kothe DB, Zemach C. 1992. A continuum method for modeling surface tension. *J. Comp. Phys.* 100:335–54

Braun RJ, McFadden GB, Coriell SR. 1994. Morphological instability in phase-field models of solidification. *Phys. Rev. E* 49:4336–52

Caginalp G. 1985. Surface tension and supercooling in solidification theory. In *Applications of Field Theory to Statistical Mechanics*, ed. L Garrido, pp. 216–26. Berlin: Springer-Verlag

Caginalp G. 1986. An analysis of a phase field model of a free boundary. *Arch. Rat. Mech. Anal.* 92:205–45

Caginalp G. 1989. Stefan and Hele-Shaw type models as asymptotic limits of the phase-field equations. *Phys. Rev. A* 39:5887–96

Cahn JW. 1961. On spinodal decomposition. *Acta Metall.* 9:795–801

Cahn JW, Hilliard JE. 1958. Free energy of a nonuniform system. I. Interfacial free energy. *J. Chem. Phys.* 28:258–67

Callen HB. 1985. *Thermodynamics and an Introduction to Thermostatics.* New York: Wiley.

Carslaw HS, Jaeger JC. 1959. *Conduction of Heat in Solids.* Oxford: Clarendon.

Chang YC, Hou TY, Merriman B, Osher S. 1996. A level set formulation of Eulerian interface capturing methods for incompressible fluid flows. *J. Comp. Phys.* 124:449–64

Chella R, Viñals J. 1996. Mixing of a two-phase fluid by cavity flow. *Phys. Rev. E* 53:3832–40

Davis HT, Scriven LE. 1982. Stress and structure in fluid interfaces. *Adv. Chem. Phys.* 49:357–454

Davis SH. 1983. Contact–line problems in fluid mechanics. *J. Appl. Mech.* 50:977–82

Delhaye JM. 1974. Jump conditions and entropy sources in two-phase systems. Local instant formulation. *Int. J. Multiphase Flow* 1:395–409

Dell'Isola F, Gouin H, Rotoli G. 1996. Nucleation of spherical shell-like interfaces by second gradient theory: numerical simulations. *Eur. J. Mech. B/Fluids* 15:545–68

Dell'Isola F, Gouin H, Seppecher P. 1995. Radius and surface tension of microscopic bubbles by second gradient theory. *C. R. Acad. Sci. Paris* 320:211–16

Dell'Isola F, Kosiński W. 1993. Deduction of thermodynamic balance laws for bidimensional nonmaterial directed continua modelling interphase layers. *Arch. Mech.* 45:333–59

de Sobrino L. 1976. Some thermodynamic and stability properties of a fluid with gradient dependent free energy. *Can. J. Phys.* 54:105–17

de Sobrino L. 1985. Note on capillary waves in the gradient theory of interfaces. *Can. J. Phys.* 63:1132–33

de Sobrino L, Peternelj J. 1982. Thermal fluctuations in the interface of an inhomogeneous fluid. *Can. J. Phys.* 60:137–53

de Sobrino L, Peternelj J. 1985. On capillary waves in the gradient theory of interfaces. *Can. J. Phys.* 63:131–34

Drazin PG, Reid WH. 1981. *Hydrodynamic Stability.* Cambridge: Cambridge Univ. Press

Dunn JE. 1986. Interstitial working and a nonclassical continuum thermodynamics. In *New Perspectives in Thermodynamics*, ed. J Serrin. Berlin: Springer

Dunn JE, Serrin JB. 1985. On the thermomechanics of interstitial working. *Arch. Rat. Mech. Anal.* 88:95–133

Dussan V EB. 1979. On the spreading of liquids on solid surfaces: static and dynamic contact lines. *Annu. Rev. Fluid Mech.* 11:371–400

Dussan V EB, Davis SH. 1974. On the motion of a fluid–fluid interface along a solid surface. *J. Fluid Mech.* 65:71–95

Felderhof BU. 1970. Dynamics of the diffuse gas-liquid interface near the critical point. *Physica* 48:541–60

Fixman M. 1967. Transport coefficients in the gas critical region. *J. Chem. Phys.* 47:2808–18

Galdi P, Joseph DD, Preziosi L, Rionero S. 1991. Mathematical problems for miscible, incompressible fluids with Korteweg stresses. *Eur. J. Mech. B Fluids* 10(3):253–67

Gibbs JW. 1876/1878. On the equilibrium of heterogeneous substances. *Trans. Conn. Acad.* 3:108–248; 3:343–524. Reprinted in 1906. *The Scientific Papers of J. Willard Gibbs*, pp. 55–371. London: Longmans, Green

Goldstein H. 1980. *Classical Mechanics*. Reading, MA: Addison-Wesley.

Gurtin ME, Polignone D, Viñals J. 1996. Two-phase binary fluids and immiscible fluids described by an order parameter. *Math. Models Methods Appl. Sci.,* 6:815.

Halperin BI, Hohenberg PC, Siggia ED. 1974. Renormalization-group calculations of divergent transport coefficients at critical points. *Phys. Rev. Lett.* 32:1289–92

Helfand E, Fredrickson GH. 1989. Large fluctuations in polymer solutions under shear. *Phys. Rev. Lett.* 62:2468–71

Hilliard JE. 1970. Spinodal decomposition. In *Phase Transformations*, ed. HI Aaronson. Metals Park, OH: Am. Soc. Metals

Hirt CW, Nichols BD. 1981. Volume of fluid (VOF) methods for the dynamics of free boundaries. *J. Comp. Phys.* 39:201–25

Hohenberg PC, Halperin BI. 1977. Theory of dynamic critical phenomena. *Rev. Mod. Phys.* 49:435–79

Huh C, Scriven LE. 1971. Hydrodynamic model of steady movement of a solid/liquid/ fluid contact line. *J. Coll. Int. Sci.* 35:85–101

Hyman JM. 1984. Numerical methods for tracking interfaces. *Phys. D* 12:396–407

Irving JH, Kirkwood JG. 1950. The statistical mechanical theory of transport processes. IV. The equations of hydrodynamics. *J. Chem. Phys.* 18:817–29

Jacqmin D. 1996. An energy approach to the continuum surface tension method. *Proc. 34th Aerosp. Sci. Meet. Exh.* AIAA 96-0858. Reno: Am. Inst. Aeron. Astron.

Jasnow D, Viñals J. 1996. Coarse-grained description of thermo-capillary flow. *Phys. Fluids* 8:660–69

Joseph DD. 1990. Fluid dynamics of two miscible liquids with diffusion and gradient stresses. *Eur. J. Mech. B Fluids* 9:565–96

Joseph DD, Huang A, Hu H. 1996. Non-solenoidal velocity effects and Korteweg stresses in simple mixtures of incompressible liquids. *Phys. D* 97:104–25

Juric D, Tryggvason G. 1995. A front-tracking method for liquid-vapor phase change. In *Advances in Numerical Modeling of Free Surface and Interfacial Fluid Dynamics*, ed. PE Raad, TT Huang, G Tryggvason, FED 234:141-48. New York: ASME

Juric D, Tryggvason G. 1996. Direct numerical simulations of flows with phase change. *Proc. 34th Aerosp. Sci. Meet. Exh., AIAA 96-0857.* Reno: Am. Inst. Aeron. Astron.

Juric D, Tryggvason G. 1997. Computations of boiling flows. *Int. J. Multiph. Flow.* In press

Karma A, Rappel W. 1997. Phase-field simulation of three-dimensional dendrites: is microscopic solvability theory correct? *J. Cryst. Growth* 174:54–64

Kawasaki K. 1970. Kinetic equations and time correlation functions of critical fluctuations. *Ann. Phys.* 61:1–56

Kittel C, Kroemer H. 1980. *Thermal Physics*. New York: Freeman

Kobayashi R. 1993. Modeling and numerical simulations of dendritic crystal growth. *Phys. D* 63:410–23

Korteweg DJ. 1901. Sur la forme que prennent les équations du mouvements des fluides si l'on tient compte des forces capillaires causées par des variations de densité considérables mais continues et sur la théorie de la capillarité dans l'hypothèse d'une variation continue de la densité. *Arch. Néerl. Sci. Exactes Nat. Ser. II* 6:1–24

Lamb H. 1932. *Hydrodynamics*. Cambridge: Cambridge Univ. Press

Landau LD, Lifshitz EM. 1959. *Fluid Mechanics*. New York: Pergamon

Langer JS. 1986. Models of pattern formation in first-order phase transitions. In *Directions in Condensed Matter Physics*, ed. G Grinstein, G Mazenko, pp. 165–86. Philadelphia: World Sci.

Langer JS, Turski LA. 1973. Hydrodynamic model of the condensation of a vapor near its critical point. *Phys. Rev. A* 8:3230–43

Lighthill J. 1978. *Waves in Fluids*. Cambridge: Cambridge University Press

Lord Rayleigh. 1892. On the theory of surface forces—II. Compressible fluids. *Phil. Mag.* 33:209–20

Lowengrub J, Truskinovsky L. 1997. Cahn Hilliard fluids and topological transitions. *Proc. R. Soc. London Ser. A*. In press

Maxwell JC. 1876. Capillary action. In *Encyclopaedia Britannica*, 9th ed. Reprinted in 1952. *The Scientific Papers of James Clerk Maxwell*, 2:541–91. New York: Dover

Mulder W, Osher S, Sethian JA. 1992. Com-

puting interface motion in compressible gas dynamics. *J. Comp. Phys.* 100:209–28

Nadiga BT, Zaleski S. 1996. Investigations of a two-phase fluid model. *Eur. J. Mech. B Fluids.* 15:885–96

Nobari MR, Jan YJ, Tryggvason G. 1996. Head-on collision of drops—a numerical investigation. *Phys. Fluids* 8:29–42

Onuki A. 1989. Elastic effects in the phase transition of polymer solutions under shear flow. *Phys. Rev. Lett.* 62:2472–75

Onuki A, Kawasaki K. 1979. Nonequilibrium steady state of critical fluids under shear flow: a renormalization group approach. *Ann. Phys.* 121:456–528

Onuki A, Yamazaki K, Kawasaki K. 1981. Light scattering by critical fluids under shear flow. *Ann. Phys.* 131:217–42

Osher S, Sethian JA. 1988. Fronts propagating with curvature-dependent speed: algorithms based on Hamilton–Jacobi formulations. *J. Comp. Phys.* 79:12–49

Poisson SD. 1831. *Nouvelle Théorie de l'Action Capillaire*, Paris: Bachelier

Rowlinson JS, Widom B. 1989. *Molecular Theory of Capillarity*. Oxford: Clarendon

Seppecher P. 1996. Moving contact lines in the Cahn-Hilliard theory. *Int. J. Eng. Sci.* 34(9):977–92

Sethian JA. 1996. *Level Set Methods* Cambridge: Cambridge Univ. Press

Siggia ED, Halperin BI, Hohenberg PC. 1976. Renormalization-group treatment of the critical dynamics of the binary-fluid and gas-liquid transitions. *Phys. Rev. B* 13:2110–23

Stanley HE. 1971. *Introduction to Phase Transitions and Critical Phenomena*. Oxford: Oxford Univ. Press

Starovoitov VN. 1994. Model of the motion of a two-component liquid with allowance of capillary forces. *J. Appl. Mech. Techn. Phys.* 35:891–97

Sussman M, Smerka P, Osher S. 1994. A level set approach for computing solutions to incompressible two-phase flow. *J. Comp. Phys.* 114:146–59

Truskinovsky L. 1993. Kinks versus shocks. In *Shock Induced Transitions and Phase Structures in General Media*, ed. JE Dunn, R Fosdick, M Slemrod, 52:185–229. New York: Springer-Verlag

Tsai W, Yue DKP. 1996. Computation of non-linear free-surface flows. *Annu. Rev. Fluid Mech.* 28:249–78

Turski LA, Langer JS. 1980. Dynamics of a diffuse liquid-vapor interface. *Phys. Rev. A* 22:2189–95

Unverdi SO, Tryggvason G. 1992a. Computations of multi-fluid flows. *Phys. D* 60:70–83

Unverdi SO, Tryggvason G. 1992b. A front-tracking method for viscous, incompressible, multi-fluid flows. *J. Comp. Phys.* 100:25–37

van der Waals JD. 1893. The thermodynamic theory of capillarity under the hypothesis of a continuous density variation. Transl. JS Rowlinson, 1979, in *J. Stat. Phys.* 20:197–244 (From Dutch, German, French)

Wang SL, Sekerka RF, Wheeler AA, Murray BT, Coriell SR, et al. 1993. Thermodynamically-consistent phase-field models for solidification. *Phys. D* 69:189–200

Warren JA, Boettinger WJ. 1995. Prediction of dendritic growth and microsegregation patterns in a binary alloy using the phase-field method. *Acta Metall. Mater.* 43:689–703

Warren JA, Murray BT. 1996. Ostwald ripening and coalescence of a binary alloy in two dimensions using a phase-field model. *Mod. Simul. Mater. Sci. Eng.* 4:215–29

Weatherburn CE. 1925. Differential invariants in geometry of surfaces, with applications to mathematical physics. *Q. J. Math.* 50:230–69

Wheeler AA, McFadden GB, Boettinger WJ. 1996. Phase-field model for solidification of a eutectic alloy. *Proc. R. Soc. London Ser. A* 452:495–525

Wheeler AA, Murray BT, Schaefer RJ. 1993. Computation of dendrites using a phase-field model. *Phys. D* 66:243–62

Yang AJM, Fleming PD III, Gibbs JH. 1976. Molecular theory of surface tension. *J. Chem. Phys.* 64:3732–47